ARTICLE

The baroreflex afferent pathway plays a critical role in H$_2$S-mediated autonomic control of blood pressure regulation under physiological and hypertensive conditions

Ying Li[1,2], Yan Feng[1,3], Li Liu[1], Xue Li[1], Xin-yu Li[1], Xun Sun[1,3], Ke-xin Li[1,3], Rong-rong Zha[1,3], Hong-dan Wang[1], Meng-di Zhang[1,4], Xiong-xiong Fan[1], Di Wu[1], Yao Fan[1], Hao-cheng Zhang[1], Guo-fen Qiao[1] and Bai-yan Li[1]

Hydrogen sulfide (H$_2$S), which is closely related to various cardiovascular disorders, lowers blood pressure (BP), but whether this action is mediated via the modification of baroreflex afferent function has not been elucidated. Therefore, the current study aimed to investigate the role of the baroreflex afferent pathway in H$_2$S-mediated autonomic control of BP regulation. The results showed that baroreflex sensitivity (BRS) was increased by acute intravenous NaHS (a H$_2$S donor) administration to renovascular hypertensive (RVH) and control rats. Molecular expression data also showed that the expression levels of critical enzymes related to H$_2$S were aberrantly downregulated in the nodose ganglion (NG) and nucleus tractus solitarius (NTS) in RVH rats. A clear reduction in BP by the microinjection of NaHS or *L*-cysteine into the NG was confirmed in both RVH and control rats, and a less dramatic effect was observed in model rats. Furthermore, the beneficial effects of NaHS administered by chronic intraperitoneal infusion on dysregulated systolic blood pressure (SBP), cardiac parameters, and BRS were verified in RVH rats. Moreover, the increase in BRS was attributed to activation and upregulation of the ATP-sensitive potassium (K$_{ATP}$) channels Kir6.2 and SUR1, which are functionally expressed in the NG and NTS. In summary, H$_2$S plays a crucial role in the autonomic control of BP regulation by improving baroreflex afferent function due at least in part to increased K$_{ATP}$ channel expression in the baroreflex afferent pathway under physiological and hypertensive conditions.

Keywords: hydrogen sulfide; hydrogen sulfide synthase; blood pressure regulation; baroreflex afferent pathway; potassium channel; protein kinase

INTRODUCTION

Hydrogen sulfide (H$_2$S), a colorless gas with a rotten egg smell, has been regarded as a toxic gas for more than a century [1]. In recent years, H$_2$S has been recognized as a novel gaseous signaling molecule along with nitric oxide (NO) and carbon monoxide (CO) [2]. Similar to NO and CO, H$_2$S is endogenously generated by *L*-cysteine by several enzymes. The three most important enzymes for the synthesis of H$_2$S in vivo are cystathionine γ-lyase (CSE), cystathionine β-synthase (CBS), and 3-mercaptopyruvate sulfurtransferase (3-MST) [3]. The expression levels of these enzymes are specific, and CSE plays a major role in the cardiovascular system. CBS is generally regarded as the major synthase in the central nervous system. It has been suggested that 3-MST contributes to the production of H$_2$S in the brain and vascular endothelium [4, 5]. H$_2$S has diverse and widespread biological functions, including its vasodilatation function and functions against endoplasmic reticulum stress, apoptosis, and inflammation [6–8]. H$_2$S also contributes to

ameliorating ventricular structural remodeling and cardiac function [9]. The methylene blue and sulfide-sensitive electrode methods have shown that plasma H$_2$S is increased or decreased in some human diseases and animal disease models. Inhibitors of H$_2$S synthase caused a decrease in measured plasma H$_2$S (i.e., stored sulfide) in animal models and also changed physiological parameters, such as blood pressure (BP), in parallel [10]. Hypertension is a major risk factor that predisposes patients to cardiovascular disorders and has high rates of morbidity and mortality. In general, H$_2$S is a vasodilator (over the short term); it relaxes vascular smooth muscle and thus can produce an antihypertensive effect [10]. CSE-knockout mice were reported to exhibit a significant increase in BP compared to that of wild-type mice [11]. The two kidneys, one clamp (2K1C, a systolic renal artery clamp) model is a useful animal model of renovascular hypertension (RVH), a common form of secondary hypertension and the most common form of curable hypertension. Lu et al. found that the administration of NaHS

(5.6 mg·kg^{-1}·d^{-1}, intraperitoneal (i.p.)) successfully reduced the development of hypertension in the 2K1C model [12]. Moreover, H₂S regulates BP via an increase in transient receptor potential vanilloid 1 (TRPV1) protein expression, leading to enhanced carotid sinus baroreceptor sensitivity [13]. Notably, the baroreceptor reflex afferent pathway consists of the solitary tract nucleus (NTS) and nodose ganglion (NG), which plays a key role in BP regulation [14, 15]. Defects in baroreflex can lead to kidney-related hypertension [16]. The ATP-sensitive potassium channel (K$_{ATP}$), which is recognized as a target for H₂S, is widely distributed in vivo [17]. It is currently believed that the K$_{ATP}$ channel is associated with baroreflex function. A study showed that vascular K$_{ATP}$ channels played a role in the increased BP variability observed in chronic sinoaortic denervation rats [18]. K$_{ATP}$ channels are composed of four pore-forming subunits (Kir6.1 and Kir6.2 encoded by KCNJ8 and KCNJ11, respectively) and four regulatory sulfonylurea receptor (SUR) ATP-binding cassette subunits (subfamily C: SUR1, SUR2A, or SUR2B) [19]. Studies have also shown that H₂S can regulate central nervous system function through the protein kinase A (PKA)/N-methyl-D-aspartate receptor (NR) pathway [20]. The neuromodulatory effect of glutamatergic transmission has been reported to be involved in baroreflex regulation [21]. Therefore, we presumed that the K$_{ATP}$ and PKA/NR pathways play an important role in the regulation of BP mediated by H₂S. In this study, we used the 2K1C method (using thin threads instead of clips) to develop a renal hypertension model [12, 22]. The effects of H₂S on BP regulation and baroreflex sensitivity (BRS) under physiological and hypertensive conditions and the underlying mechanisms were studied.

MATERIALS AND METHODS

Chemicals
Sodium hydrosulfide (NaHS, 161527 Lot# SHBF1745V), L-cysteine (#C7352), glibenclamide (Gli, a selective antagonist for the ATP-sensitive potassium channel, #G0639), phenylephrine (PE, # P1250000) and sodium nitroprusside (SNP, #228710) were all purchased from Sigma (St. Louis, MO, USA). The drugs were dissolved in a suitable solvent prior to use.

Animal procedures
The Institutional Animal Care and Use Committee of Harbin Medical University approved all protocols regarding the animals used in experiments, and these protocols were in accordance with the recommendations of the Panel on Euthanasia of the American Veterinary Medical Association and the National Institutes of Health Publication "Guide for the Care and Use of Laboratory Animals" (http://www.nap.edu/readingroom/books/labrats/). All rats were purchased from the Animal Center of the Second Affiliated Hospital, Harbin Medical University (animal certificate number, SCXK (Hei) 2019-001) and bred in our animal facility. All rats were housed in a specific pathogen-free facility maintained at 23–25 °C with 5 rats per cage under a 12 h light-12 h dark cycle and given a standard rodent diet and water ad libitum.

Age-matched normal adult and RVH male Sprague-Dawley (SD) rats weighing 220–250 g were used to collect tissues from the NG and NTS and molecular expression studies to assess protein expression in this study. Rats were randomly grouped for each experiment. The rats were anesthetized with the i.p. administration of 3% amobarbital sodium at a dose of 25 mg·kg^{-1} during the experiment and sacrificed at the end of the experiment. BP and BRS were monitored long term in vivo with or without NaHS administration. While NaHS was microinjected into the NG, the arterial pressure was monitored to test the drugs' effects. Systolic BP (SBP) was measured by the tail-cuff method (BP-98A, Saffron, Japan) weekly after renal artery stenosis. BRS was evaluated by measuring the response of the heart rate (HR) and mean arterial

pressure (MAP) to PE/SNP; the corresponding data are presented as ΔHR in bpm and ΔMAP in mmHg, respectively.

Renovascular hypertension modeling
The traditional 2K1C model uses a U-shaped silver clip with the same diameter as the left renal artery cuff of the rat; however, the silver clip is difficult to make and expensive, and more importantly, the inner diameter when a U-shaped silver clip is used is difficult to control. As described in the literature [22], we used silk thread to directly narrow the renal artery of the left kidney, which is a widely accepted procedure to establish the RVH rat model. In addition, this method is simple to operate and causes fewer difficulties than the 2K1C method, as mentioned above. Rats with an average SBP more than 20 mmHg above baseline BP (~115 mmHg before treatment in the current experiment) were considered successfully established RVH model rats. Seven weeks after establishment of the RVH rat model with unilateral renal artery stenosis, the rats were anesthetized with i.p. 3% amobarbital sodium (25 mg·kg^{-1}) and placed in a lateral position. For rats in the RVH and RVH + NaHS groups, the unilateral flank was shaved, cleaned by chlorhexidine scrub, and then disinfected with 70% ethanol. The left kidney was exposed, and the left kidney artery was ligated with a silk thread. The skin was successively closed with 4–0 absorbable sutures and treated with povidone–iodine (7.5%) for disinfection. Penicillin (80,000 units) was also given via intramuscular injection [23]. Sham control rats were also prepared under the same procedures without ligation. After recovering from anesthesia, the animals were monitored for at least 30 min to ensure that there was no bleeding from the surgical area and then returned to the clean animal facility. The SBP of the rats in each group was recorded weekly.

Acute intravenous NaHS injection in RVH rats
At 4 weeks after renal artery ligation or sham surgery, the anesthetized rats were fitted with femoral artery and vein catheters to record MAP and administered the individual drugs. After intravenous NaHS (0.67 mg·kg^{-1}) or 0.9% sterile saline (Ctrl) injection, MAP was continuously monitored for 1 h. Meanwhile, the BRS induced by PE (10 μg·kg^{-1}) was tested before (BRS baseline) and after injections over 10–60 min in RVH and control rats.

Chronic intraperitoneal infusion of NaHS in RVH rats
To examine the therapeutic effect of H₂S after the development of RVH, rats were subjected to i.p. infusions of 0.9% sterile saline or NaHS (5.6 mg·kg^{-1}·d^{-1}, RVH + NaHS) for an additional 4 weeks at 4 weeks after renal artery ligation [12]. Meanwhile, the control rats were simultaneously subjected to infusions of 0.9% sterile saline or NaHS (5.6 mg·kg^{-1}·d^{-1}, Ctrl + NaHS). The blocker group was injected with glibenclamide (Gli, 5 mg·kg^{-1}·d^{-1}) before the i.p. injection of NaHS [24].

Blood pressure measurement
The SBP of all rats was measured noninvasively weekly. A manometer-tachometer (BP-2010E, Softeron Biotechnology, Beijing, China) was used to measure the SBP of conscious rats by the tail-cuff method.

Echocardiographic measurements
Transthoracic echocardiography with an ultrasound machine (Vevo 2100 imaging system, VisualSonics, Toronto, Canada) was used to evaluate the cardiac function of the rats. The left ventricular systolic/diastolic internal diameter (LVIDs/LVIDd, mm), interventricular septum systolic/diastolic thickness (IVSs/IVSd, mm), and left ventricular systolic/diastolic posterior wall (LVPWs/LVPWd, mm) were measured, and the ejection fraction (EF, %) and fractional shortening (FS, %) were calculated from recordings in short axis (SAX) or parasternal long axis mode.

Baroreflex sensitivity detection

Rats were anesthetized with i.p. 3% amobarbital sodium (25 mg·kg^{-1}) and cannulated, after which the femoral artery was connected to a physiological pressure transducer (AD Instruments MLT844, Norway) with LabChart 7 software, which can automatically and simultaneously monitor changes in MAP and HR. PE or SNP at three different doses (1, 3, and 10 μg·kg^{-1}) was injected by an indwelling venous catheter to induce transient changes in BP and HR. The maximal and baseline HR and MAP values were recorded for all rats in each group. BRS, defined as the ratio of ΔHR/ΔMAP, was calculated for each dose of PE and SNP.

Nodose ganglia microinjection

After the rats had relaxed and the femoral artery was cannulated via the procedures above, the baseline arterial BP before neck surgery was routinely monitored. Immediately, the left side NG was dissected with caution as we previously described [25, 26] and then punctured by using a specifically designed glass syringe (Hamilton, Reno, NEV, USA) affixed with a half-inch 30G stainless steel syringe needle. Both the HR and MAP were collected during NG microinjection by using LabChart 7 software.

Quantitative RT-PCR (qRT-PCR)

One mRNA sample collected was extracted from each NG or NTS tissue from 2 or 3 rats, and duplicate tests were performed using one mRNA sample in the same group (Ctrl or RVH). Total RNA was extracted using TRIzol reagent (Invitrogen, Carlsbad, CA, USA) according to the manufacturer's instructions. cDNA was synthesized using the Reverse Transcription Kit (Applied Biosystems) and SYBR Green PCR Master Mix Kit (Applied Biosystems) with the listed PCR primers (Supplementary Table S1). The primer sequences for 3-MST, Kir6.1/6.2, SUR1/2, and GAPDH were mined from previously published literature, the CSE and CBS primers were designed by Sangon Biotech Corporation (Shanghai, China), and the PKA primer set was designed by Wcgene Biotech Corporation (Shanghai, China). qRT-PCR experiments were run on a LightCycler® 96 PCR System (Roche). The 2$^{-\Delta\Delta Ct}$ method was applied for data analysis.

Western blot analysis

For each sample, NG/NTS tissues were extracted from 2–3/1–2 rats and lysed by RIPA buffer. Protein extracts (100 μg per sample, as assessed through a BCA protein assay) were subjected to 10% SDS-Tris glycine gel electrophoresis and then transferred (Mini PROTEAN, Bio-Rad Laboratories, Shanghai, China) to a nitrocellulose membrane. The membrane was blocked with 5% nonfat dry milk at 4 °C overnight, followed by another overnight incubation at 4 °C with the primary antibody (Supplementary Table S2). The membrane was then incubated with the secondary antibody (against mouse) at room temperature for 55 min. The results were detected and analyzed via an Odyssey system (LI-COR Biosciences, Lincoln, NE, USA).

Data analysis

We conducted data analysis in a blinded fashion whenever possible and set proper controls for every experimental protocol. No sample calculation was carried out. The numbers of rats and independent experiments run are described in the figure legends. Excel (Microsoft, Northampton, MA, USA) was used for statistical analysis. Trace filtering and graphing of the data were accomplished with Origin (Microsoft). Statistical analysis was undertaken only for studies in which each group size was at least five. For all experiments (in vivo), the number of observations (group size) is provided in the figure legend and a minimum of five independent observations were carried out. The exact size (*n*) for each experimental group/condition is provided, and "*n*" refers to independent values, rather than replicates. The declared group size is the number of independent values, and statistical analysis was performed using these independent values. qRT-PCR or Western blot measurements were performed in duplicate, and an average was taken for each sample and used to calculate the final mean data. Two-tailed paired or unpaired Student's *t* test was applied to compare the significance of differences before and after the treatment or between the groups. When *F* values reached the level of statistical significance required and no significant variance in homogeneity was observed, one-way ANOVA followed by Tukey's post hoc test was used to compare the groups. To reduce unwanted sources of variation by data normalization in qRT-PCR and Western blot data analyses, the value for each control and test group was "normalized" to the mean value for the control group, and the unit for such normalized data is the fold change compared to the mean value of the control group. Figure legends have been appropriately labeled to reflect this. The averaged data are presented as the mean ± SD. A *P* value ≤0.05 was used to indicate a statistically significant difference.

RESULTS

Acute effect of H₂S on BRS under physiological and hypertensive conditions

To determine whether H₂S would have a direct effect on BRS, which is associated with the baroreflex afferent pathway, we tested the BRS by measuring the MAP in the presence of PE; meanwhile, the electrocardiogram was monitored accordingly. The results showed that BRS was dramatically elevated by acute NaHS (H₂S) injections (i.v.) in both normal control and RVH model rats (Fig. 1a). In the control rats, the BRS peaked at 40 min after treatment and was restored to near the control level at 60 min after treatment. In RVH rats, the times at which BRS peaked recovered were 10 and 20 min earlier, respectively than those of the control group (Fig. 1b). Importantly, the elevated BRS observed in control rats at all timepoints was significantly higher than that in the RVH model rats over the observation period.

Gene and protein expression of hydrogen sulfide synthase in the NG and NTS

Since H₂S participates in BRS modification via the baroreflex pathway, we then explored the presence of endogenous H₂S synthase in the NG and NTS, key parts of the baroreflex afferent pathway that house the cell bodies of 1st- and 2nd-order baroreceptor and baroreceptive neurons to generate H₂S. Our qRT-PCR results showed that three synthases, CSE, CBS, and 3-MST, were expressed in the NG and NTS (Supplementary Fig. S1). Moreover, compared with their levels in control rats, levels of all three synthases were reduced in the NG or NTS (Fig. 2a, b) in RVH model rats. Taking into account the amount of its expression revealed by the cycle number and the importance of this enzyme in cardiovascular disorders such as hypertension and infarction, CSE was selected for the next immunoblotting experiment [27, 28]. Similar to the qRT-PCR data, the immunoblotting data showed that RVH modeling downregulated CSE protein expression at the tissue level in the NG and NTS compared with that in control rats (Fig. 2c, d), suggesting that this is the most likely cause for the reduction in BRS in RVH rats.

Changes in blood pressure caused by the microinjection of H₂S or L-cysteine into the nodose ganglion (NG) under physiological and hypertensive conditions

To determine the effect of H₂S on BP regulation, changes in the MAP were investigated when NaHS or L-cysteine was microinjected directly into the NG, and the results showed that NaHS dramatically decreased BP in a dose-dependent manner in both control and RVH model rats (Fig. 3a). Further analysis revealed that the higher the concentration of NaHS was the longer the observed duration of action was (Supplementary Fig. S2). The half-maximal
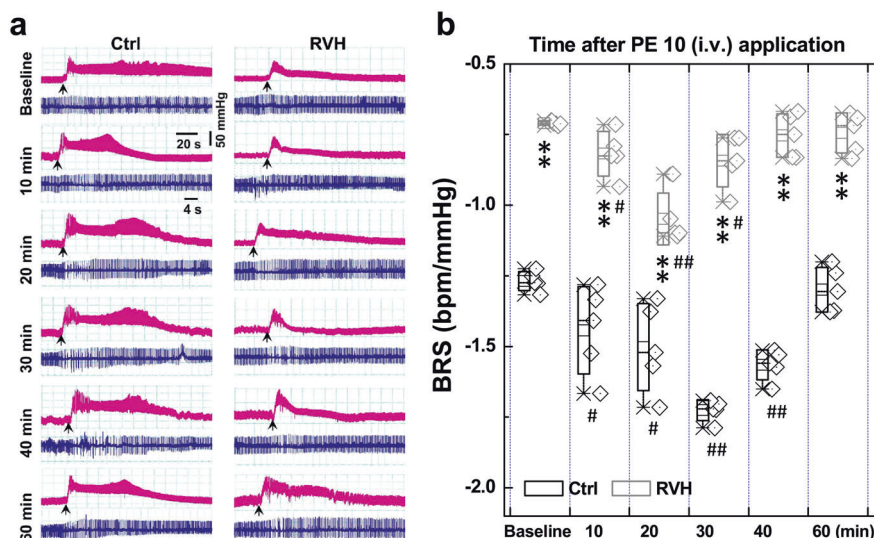
Fig. 1 Acute effect of NaHS on baroreflex sensitivity (BRS) under control and hypertensive conditions (renovascular hypertension, RVH). A femoral artery catheter was connected to a transducer to measure the change in MAP, and a venous cannula was used to administer NaHS and PE. **a** Representative recordings of MAP collected from control (Ctrl, $n = 5$) and RVH ($n = 5$) rats in the presence of 10 μg·kg⁻¹ PE before (baseline) and after (10–60 min) the intravenous injection of 0.67 mg·kg⁻¹ NaHS. Representative recordings of heart rate (HR) along with changes in blood pressure (BP). **b** The summarized changes in BRS (ΔHR/ΔMAP, bpm/mmHg) upon treatment with PE (10 μg·kg⁻¹) before (baseline) and after (10–40 min) NaHS injection. The averaged data are expressed as the mean ± SD. *$P < 0.05$ and **$P < 0.01$ vs. baseline of the Ctrl or model group; #$P < 0.05$ and ##$P < 0.01$ vs. the Ctrl group.
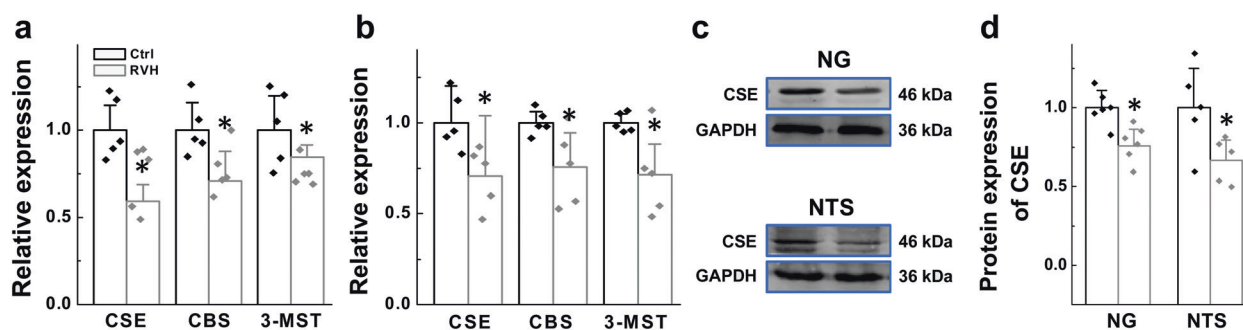

Fig. 2 Gene and protein expression of enzymes responsible for hydrogen sulfide synthesis (CBS, CSE, and 3-MST) in the nodose ganglia (NG) and nucleus tractus solitarius (NTS). Relative mRNA expression levels of CSE, CBS, and 3-MST in the NG (**a**, $n = 5$ duplicates/group) and NTS (**b**, $n = 5$ duplicates/group) from Ctrl and RVH rats were measured by PCR. (**c**, **d**) The representative bands and expression levels of the CSE (CTH) protein in NG ($n = 5$ duplicates/group) and NTS ($n = 5$ duplicates/group) from Ctrl and RVH rats were measured by Western blot analysis, and the data are presented as fold change values normalized to control values. The results were analyzed using two-tailed unpaired Student's t-test, and averaged data are expressed as the mean ± SD, *$P < 0.05$ vs. the Ctrl group.

effective concentration (EC₅₀) was increased by approximately fourfold (~374 μM for RVH model rats vs. ~88 μM for control rats) (Fig. 3b). Similarly, a dose-dependent reduction in BP was also confirmed after microinjection of L-cysteine into the NG, and the EC₅₀ was increased almost three times from ~3.6 mM in control rats to ~12 mM in RVH model rats (Fig. 4a, b).

Cardiovascular effects of long-term intravenous H₂S administration to normal and hypertensive model rats
To further test the antihypertensive action of H₂S, a long-term experiment involving different treatments was conducted, and our preliminary data showed that the SBP was significantly increased compared to that in control rats and peaked at 3 or 4 weeks after renal artery ligation; furthermore, this increase in SBP was maintained over the 8 weeks observation period. Based on this model, NaHS was administered by i.p. injection for 4 consecutive weeks, and the results showed that NaHS did not change the SBP of normal control rats. However, NaHS significantly reduced the SBP in conscious RVH model rats (Fig. 5) at 1 week after NaHS

administration, and the SBP decreased back to the control level at 2 week after NaHS application. Furthermore, there was no difference in body weight among the groups (Table 1).

H₂S has been documented to have a protective effect on the heart [29, 30]. Consistently, the echocardiographic results showed that H₂S did not influence any of the cardiac parameters examined in control rats. In RVH rats, SAX M-mode imaging indicated an increased LVAWd and LVAWs compared with those of the control rats (Fig. 6b, c), rather than the ratio of heart weight to body weight (HW/BW, Supplementary Fig. S3), and the increased LVAWd and LVAWs were clearly restored to near control level after NaHS treatment (Fig. 6a–c; Table 2). In addition, we suspected that NaHS may protect against kidney fibrosis through kidney contrast maps (Supplementary Fig. S4). These data strongly suggest that the acute administration of NaHS undoubtedly increased BRS through the modification of baroreflex afferent function. Similarly, the chronic administration of NaHS also increased BRS in RVH rats without significantly affecting BRS in normal control rats (Fig. 6d–f).
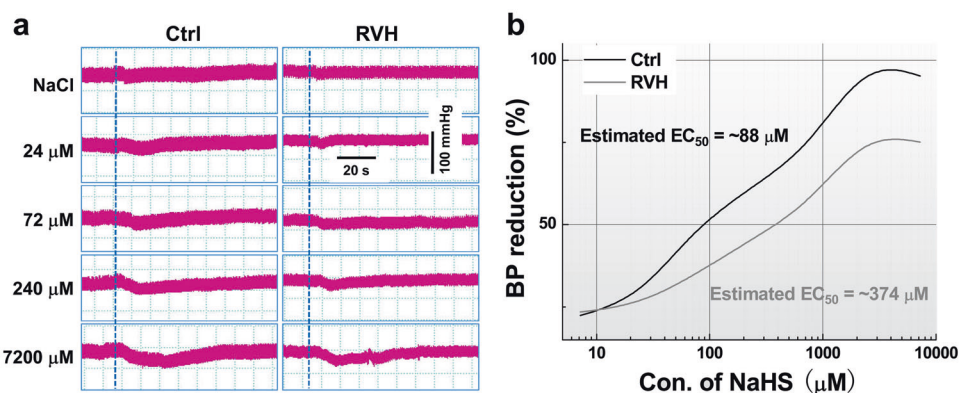
Fig. 3 **Changes in blood pressure by the microinjection of NaHS into the NG under physiological and hypertensive conditions (concentration-dependent effects of NaHS on blood pressure by NG microinjection).** a Representative BP recordings before and after the administration of saline (top) and NaHS at various doses (24, 72, 240, and 7200 μM, 0.3 μL) to control (left) and RVH (right) rats. The dashed line indicates the time at which treatment began. b Recording of the change in BP after the administration of NaHS at different doses (7.2, 24, 72, 240, 720, 2400, and 7200 μM, 0.3 μL). With the NaHS concentration as the abscissa and the percentage of BP reduction as the ordinate, dose-effect relationship curves for NaHS in Ctrl (black curve, $n = 5–7$ rats/group) and RVH (grey curve, $n = 5$ or 6 rats/group) rats were established. EC_{50}: concentration that provides 50% of the maximal effect.
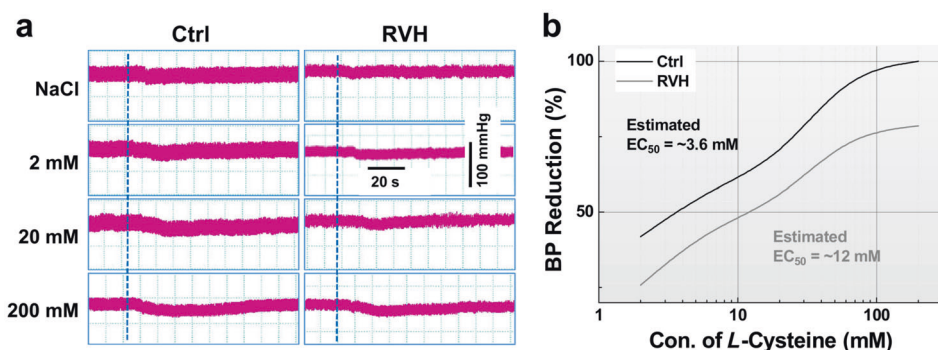

Fig. 4 **Concentration-dependent effects of *L*-cysteine on blood pressure by microinjection into the NG.** a Representative BP recordings before and after the administration of saline (top) and *L*-cysteine at different doses (2, 20, and 200 mM, 0.2 μL) in Ctrl (left) and RVH (right) rats; the dashed line indicates the time at which treatment began. b Representative recordings of BP before and after the administration of *L*-cysteine at different doses (2, 6, 20, 60, 200 mM, 0.2 μL). With the *L*-cysteine concentration used as the abscissa and the percentage of BP reduction used as the ordinate, the dose-effect relationship curves for *L*-cysteine in Ctrl (black curve, $n = 5–7$ rats/group) and RVH (grey curve, $n = 5$ or 6 for rats/group) rats were established.
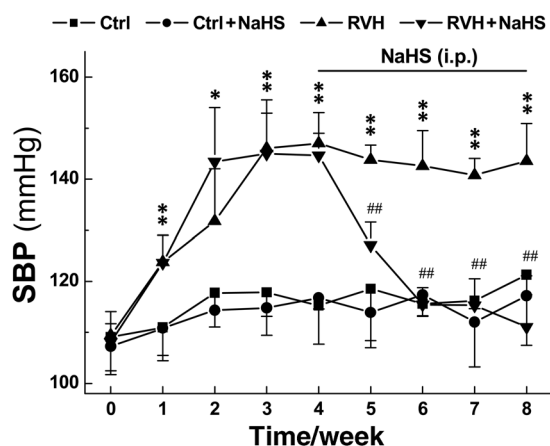

Fig. 5 **Effect of H₂S on blood pressure in normal and hypertensive model rats.** NaHS (5.6 mg·kg⁻¹·d⁻¹) was applied intraperitoneally (i.p.) for 4 weeks, and the noninvasive SBP (mmHg) of Ctrl, Ctrl + NaHS, RVH, and RVH + NaHS rats was measured weekly. Averaged data are presented as the mean ± SD; $n = 6$ rats/group. $*P < 0.05$ and $**P < 0.01$ vs. the data at time 0, $^{##}P < 0.01$ vs. the RVH group.

Table 1. Body weight in Ctrl and RVH rats before and after treatment with NaHS.

Groups	Ctrl ($n = 5$)	RVH ($n = 5$)	Ctrl + NaHS-4w ($n = 5$)	RVH + NaHS-4w ($n = 5$)
Body weight (g)	265.8 ± 14.7	257.3 ± 8.6	267.9 ± 14.6	262.7 ± 10.13

H₂S-mediated PKA-NR1 signaling in the NG and NTS

Previous studies demonstrated that the PKA-NMDAR1 (NR1) pathway is the key signaling pathway in neuromodulation and that PKA is a target of H₂S [31]. Thus, within the current working model, we tested the mRNA level of PKA in the NG and NTS. Our data showed that the expression level of PKA was significantly higher in RVH model rats than in the control rats and this change in the expression pattern was reversed by NaHS treatment (Supplementary Fig. S5). Consistent with the qRT-PCR data, the protein expression of PKA (Fig. 7a) and phosphorylation of NR1 (p-NR1, Fig. 7b) were significantly higher in RVH rats than in control rats, and these effects were abolished in the presence of NaHS. Interestingly, H₂S-mediated changes in PKA and p-NR1 expression were not detected in normal rats (Fig. 7a, b), suggesting that PKA
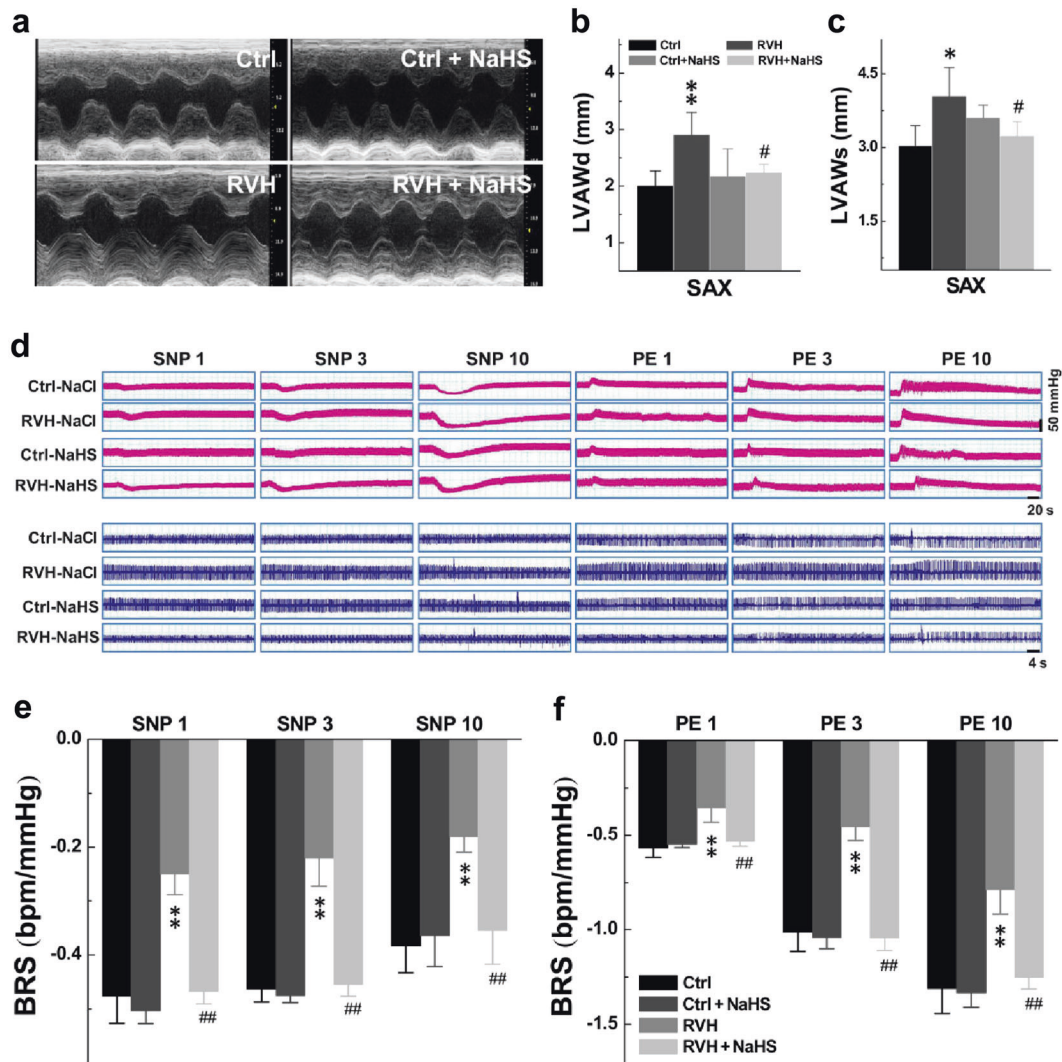
Fig. 6 **Cardiovascular effects of long-term intravenous H₂S administration in normal and hypertensive model rats. a** Image showing the cardiac morphology of Ctrl, Ctrl + NaHS (4 weeks), RVH, RVH + NaHS (4 weeks) rats in the SAX model. **b, c** Diastolic LVAW (LVAWd, mm; $n = 5$ rats/group) and systolic LVAW (LVAWs, mm; $n = 5$ rats/group). Averaged data are presented as the mean ± SD; $*P < 0.05$ and $**P < 0.01$ vs. the Ctrl group, $^{\#}P < 0.05$ vs. the RVH group. **d** Representative recordings of the MAP collected from rats in the presence of 1, 3, and 10 μg·kg⁻¹ PE or SNP. Representative recordings of the heart rate (HR) along with changes in blood pressure (BP). **e, f** Summarized changes in BRS (ΔHR/ΔMAP, bpm/mmHg) upon treatment with PE followed by SNP at different concentrations in each group are shown. Averaged data are presented as the mean ± SD; $n = 5$ rats/group. $**P < 0.01$ vs. the Ctrl group, $^{\#\#}P < 0.01$ vs. the RVH group.

Table 2. Ultrasound parameters of cardiac performance in Ctrl and RVH rats before and after treatment with NaHS.

SAX M-Model parameters	Ctrl ($n = 5$)	RVH ($n = 5$)	Ctrl + NaHS-4w ($n = 5$)	RVH + NaHS-4w ($n = 5$)
LVAWd	2.00 ± 0.27	2.91 ± 0.39**	2.18 ± 0.48	2.24 ± 0.15†
LVAWs	3.05 ± 0.4	4.05 ± 0.58*	3.61 ± 0.26	3.24 ± 0.29†
LVIDd	5.54 ± 0.83	5.44 ± 0.53	5.75 ± 0.47	5.93 ± 0.39
LVIDs	2.25 ± 0.68	2.46 ± 0.44	2.56 ± 0.57	2.90 ± 0.39
LVPWd	1.80 ± 0.22	2.34 ± 0.53	2.33 ± 0.41	1.96 ± 0.16
LVPWs	3.35 ± 0.31	3.40 ± 0.49	3.69 ± 0.24	3.05 ± 0.38
EF(%)	88.2 ± 6.06	85.2 ± 4.46	84.7 ± 7.01	80.3 ± 7.81
FS(%)	60.0 ± 8.11	55.4 ± 5.42	55.7 ± 8.89	51.2 ± 4.58

All data were presented as mean ± SD, $*P < 0.05$ and $**P < 0.01$ vs. Ctrl, $^{†}P < 0.05$ vs. RVH group.
Ctrl control rats, *RVH* renal vascular hypertension rats, *NaHS* NaHS by intraperitoneal injection for 4 weeks (4w), *EF* ejection fraction, *FS* fractional shortening, *LVAWs/LVAWd* systolic/diastolic left ventricular anterior wall, *LVIDs/LVIDd* systolic/diastolic left ventricular internal diameter, *LVPWs/LVPWd* systolic/diastolic left ventricular posterior wall, *SAX* short axis.
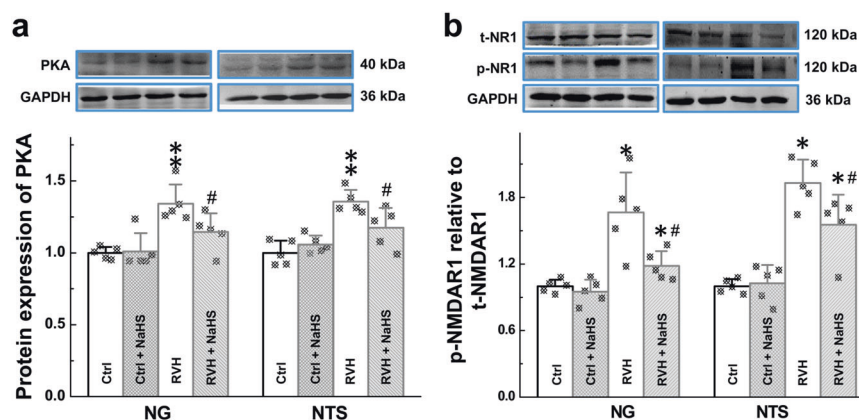
Fig. 7 H2S-mediated neurocontrol of BP regulation via PKA-NR1 signaling. a Relative protein expression of PKA in the NG ($n = 5$ duplicates/group) and NTS ($n = 6$ duplicates/group) was measured from Ctrl, Ctrl + NaHS, RVH, and RVH + NaHS rats by Western blotting. Gray value analysis was performed to quantify PKA. **b** The relative protein expression of p-NR1 and t-NR1 (p-, phosphorylated; t-, total) in the NG ($n = 5$ duplicates/group) and NTS ($n = 5$ duplicates/group) was measured from Ctrl, Ctrl + NaHS, RVH, and RVH + NaHS rats by Western blotting. Gray value analysis was performed to quantify p-NR1 and t-NR1, and the data are presented as the fold change after normalization to control values. Averaged data are expressed as the mean $\pm$ SD, *$P < 0.05$, **$P < 0.01$ vs. the Ctrl group; #$P < 0.05$ vs. the RVH group.

and p-NR1 may be key players in the development of hypertension.

H2S mediates neurocontrol of BP regulation by activating ATP-sensitive K+ channels (Kir6.2 and SUR1)
Our previous dataset showed that H2S reversed the impairment of BRS and improved BP under hypertensive conditions. Increasing evidence has shown that the K_{ATP} channel is an important target of H2S [32]. We next asked whether the K_{ATP} channel is also involved in this process. Based on the above model, glibenclamide (Gli), which blocks K_{ATP} channels, was applied (5 mg·kg^{-1}·d^{-1}, i.p.) before the i.p. injection of NaHS. The BP of these rats was almost identical to that of rats in the RVH group at the tested points, suggesting that Gli itself and DMSO (the solvent of Gli) did not exert any effects. However, the antihypertensive effect of H2S observed in the RVH + NaHS group was significantly but partially blocked by Gli (Fig. 8a). We then tested the effect of NaHS on BRS and baroreflex afferent function with or without Gli. As we expected, BRS was markedly increased in RVH model rats after 4 week of NaHS administration, and this effect was partially blocked by Gli pretreatment (Fig. 8b, c). To exclude the potential effects of NaCl and DMSO and the blocking effect of Gli, they were applied before NaHS was microinjected into the NG, and any changes in BP were simultaneously monitored. A clear and significant difference in BP was not detected among the rats administered solvents and Gli. However, after Gli treatment, the H2S-mediated reduction in BP was partially blocked, but this was not observed in the solvent-treated groups (Fig. 8d, e). Intriguingly, the in vivo observations mentioned above were consistent with the findings of our molecular expression analysis and qRT-PCR, which showed that the mRNA expression levels of both Kir6.1/6.2 and SUR1/2 in the NG and NTS were dramatically downregulated (Supplementary Fig. S6) in RVH model rats compared with control rats. Further study via immunoblotting also showed a similar change in expression of the Kir6.2 and SUR1 genes in tissues from the NG and NTS of RVH rats, and this downregulation was reversed after treatment with NaHS in the NG (Fig. 8f) and NTS (Fig. 8g).

DISCUSSION
The disorder of sympathetic and parasympathetic cardiovascular regulation is one of the most widely accepted and tested hypotheses for cardiovascular diseases. Sympathetic hyperactivity

is likely accompanied by an impaired vagal influence on the heart, in which the baroreflex mechanism is thought to be particularly important in stabilizing BP [33]. It is now commonly believed that increased sympathetic activity is associated with hypertension due to early damage to the baroreflex, which reduces the inhibition of sympathetic activity. BRS, the sensitivity with which BP changes to reflexive heart rate changes, is mainly an indicator of vagal regulation. BRS is first reduced and aggravated with disease progression in renal hypertension [34]. Notably, H2S improves carotid sinus baroreflex by inhibiting endoplasmic reticulum stress and L-type Ca^{2+} channels as well as activating TRPV1 and NMDA [13, 35–37]. Compared with the carotid sinus baroreflex, the aortic arch baroreflex has a more important role. However, thus far, few studies have examined the relationship between H2S and the function of aortic arch baroreceptors, especially the baroreflex afferent function, mainly due to technique limitations, so more evidence to extend our understanding of how H2S participates in autonomic control of BP regulation is fundamental. Herein, for the first time, our study has demonstrated that H2S achieves control of BP regulation by upregulating the K_{ATP} channel in the NG and NTS (baroreflex afferent pathway, Fig. 9).

Renovascular hypertension is a common form of secondary hypertension and the most prevalent form of curable hypertension from a clinical point of view. Our research group has performed some research in a model of RVH and found that baroreflex afferent function was indeed impaired. Interestingly, through a large number of studies, H2S and RVH have been found to be closely related, and H2S may inhibit renin activity by decreasing the synthesis and release of renin, suggesting the potential therapeutic value for H2S. Therefore, the RVH rat model can be used to accurately evaluate the effect and potential mechanism of H2S on BRS and BP, which is the major reason why we selected this RVH model to explore the relationship between H2S and baroreflex afferent function from a new perspective. It is generally accepted that the initial stages of 2K1C hypertension are primarily mediated by renin, whereas volume overload and sympathoexcitation play a more prominent role in the late phase [38, 39]. At the time of sympathetic nerve activity recording at 3 weeks after clipping, it is believed that the initial renin/aldosterone-dependent phase of hypertension has passed and that hypertension is instead primarily maintained by increased sympathoexcitatory drive [40]. The arterial baroreflex has been shown to be an inhibitory reflex with control over sympathetic drive and heart rate at rest. Herein, the renovascular hypertensive rat model was selected since this model shows significant
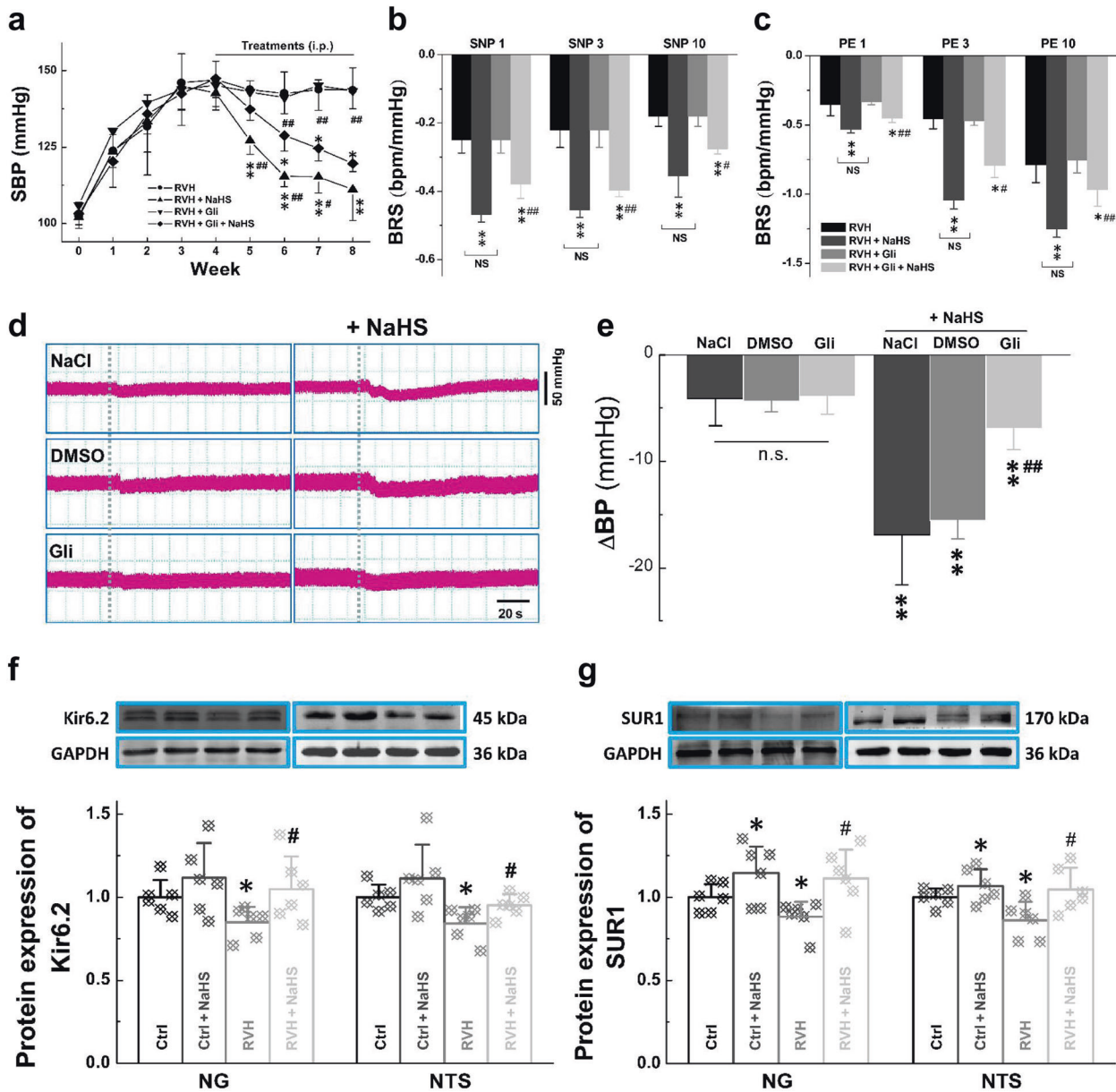
Fig. 8 **Expression of H₂S-mediated ATP-sensitive K⁺ channels (Kir6.2 and SUR1) in the NG and NTS. a** The noninvasive systolic SBP (mmHg) was measured weekly from RVH, RVH + NaHS, RVH + Gli, and RVH + Gli + NaHS rats. Averaged data are presented as the mean ± SD. $n = 5$ rats/group. *$P < 0.05$ and **$P < 0.01$ vs. the RVH group, #$P < 0.05$ and ##$P < 0.01$ vs. the RVH + Gli + NaHS group. **b, c** Summarized changes in BRS (ΔHR/ΔMAP, bpm/mmHg) upon treatment with PE followed by SNP at different concentrations in each group. $n = 5$ rats/group. **$P < 0.01$ vs. the RVH group, #$P < 0.05$ and ##$P < 0.01$ vs. the RVH + NaHS group. n.s.: no significance. **d, e** Effect of the K$_{ATP}$ channel blocker Gli on H₂S-mediated transient hypertension; blood pressure (BP) was measured before and after pretreatment (Gli, 1.5 μg/kg, a K$_{ATP}$ channel inhibitor; NaCl; DMSO) and NaHS (100 μM) treatment by microinjection into the NG. The change in BP after administration of the drugs was recorded. Averaged data are presented as the mean ± SD. $n = 7$ rats/group. **$P < 0.01$ vs. the corresponding pretreatment group; ##$P < 0.01$ vs. the DMSO + NaHS group. **f, g** Western blot analysis of Kir6.2 and SUR1 protein expression in the NG ($n = 6$ duplicates/group) and NTS ($n = 6$ duplicates/group) from Ctrl, Ctrl + NaHS, RVH, and RVH + NaHS rats. Gray value analysis was performed to quantify Kir6.2 and SUR1, and the data are presented as a fold change after normalization to control values. Averaged data are expressed as the mean ± SD; *$P < 0.05$ vs. the Ctrl group; #$P < 0.05$ vs. the RVH group.

hypertension with impaired BRS. Pharmacotherapeutic experiments in vivo also revealed the beneficial effects of chronic i.p. infusion of NaHS on BP and BRS in RVH rats. In addition, hypertension-associated cardiac remodeling is an initial adaptive process in hypertension [41]. We found that the LVAW (d/s) were markedly increased in RVH rats and improved by chronic NaHS infusion. Therefore, the reduction of BP by chronic NaHS treatment may be induced by BRS improvement without the exclusion of other mechanisms of action, which, subsequently,

improves cardiac function (LVAW) due to improved BRS and a lower BP.

Studies have shown that H₂S may play a crucial role in the pathogenesis and development of hypertension in humans. In patients with grade 2 and 3 hypertension, the plasma H₂S concentration has been found to be lower than that in healthy subjects with a normal BP [42]. In patients with portal hypertension and pulmonary hypertension, the level of H₂S and expression of CSE have also been found to be lower than those in healthy subjects
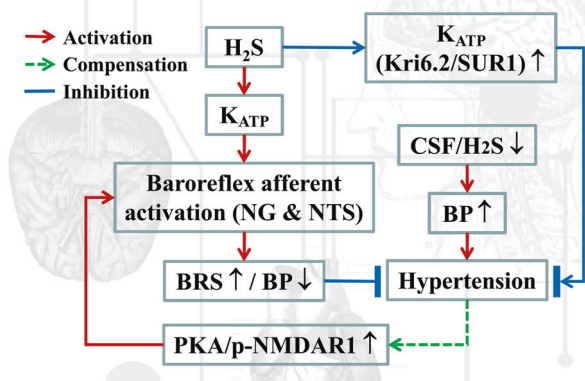
Fig. 9 Schematics of the working hypothesis. In the current working model, hydrogen sulfide (H$_2$S) directly contributes to upregulation of the K$_{ATP}$ channel, which improves baroreflex afferent function and BP regulation.

with a normal BP [43, 44], strongly implying the contribution of CSE/H$_2$S deficiency to BP augmentation [45]. The existing evidence has shown that the level of H$_2$S in the plasma/urinary and gene expression and activity of CSE in the thoracic aorta are also suppressed in SHRs [45]. Interestingly, our current observations are consistent with these existing data and have demonstrated the direct participation of the baroreflex afferent pathway in H$_2$S-mediated autonomic control of circulation, i.e., dramatic downregulation of the functional expression of CSE at both the gene and protein levels in the baroreflex afferent pathway (NG/NTS) under hypertensive conditions, which is the likely reason for the impairment of BRS and BP homeostasis in RVH.

Since the NG and NTS play an important role in the baroreflex, the direct activation of 1st-order baroreceptor neurons within the baroreflex afferent pathway by the microinjection of H$_2$S into the NG is also worth exploring. Previous studies have confirmed that H$_2$S regulates cardiovascular activity through central mechanisms [46]. Interestingly, it was shown that unilateral microinjection of NaHS into the NTS caused transient and dose-dependent hypotension [47]. Importantly, an exactly inverse effect on BP by direct activation of the 1st- and 2nd-order neurons in the NG and NTS was reported [48, 49]. Therefore, based upon our previous observation, we suspected that H$_2$S may also induce presser or depressor responses via direct administration of H$_2$S into the NG [50]. As expected, H$_2$S-mediated BP reduction in a dose-dependent manner was confirmed by microinjection, and this BP reduction was more dramatic in normal rats with a lower EC$_{50}$ than in RVH rats. This series of concentrations were selected for two main reasons. First, theoretically, administered NaHS cannot be completely converted into H$_2$S, and it is difficult to know the proportion of NaHS converted to H$_2$S in vivo. Studies have shown that 2000 μM NaHS can be unilaterally microinjected into the CVLM. Therefore, we hypothesized that the application of NaHS to the periphery may increase the concentration appropriately due at least in part to potential leakage during microinjection because of tiny nodose ganglion tears in the injection site. Second, as we focused on the effects of H$_2$S on BP and its potential mechanisms, so we chose to use H$_2$S at a wider range of concentrations to determine the maximal effect of H$_2$S on BP. When concentrations for therapeutic use are considered in the future, more attention needs to be paid to the differential toxicity of H$_2$S on different cells, organs, and systems in our future investigation. Furthermore, H$_2$S-induced BP reduction was mimicked by the microinjection of L-cysteine and NaHS with equal efficacy. These data imply that the NG plays a role in the autonomic control of BP regulation similar to that of NTS and that synergistic hypotension was mediated by H$_2$S both centrally and peripherally. It stands to reason that an

impaired baroreceptor (reduced neuroexcitability) may be responsible for the decreased sensitivity of the NG to H$_2$S under hypertensive conditions, presumably due to the conversion of less NaHS to H$_2$S resulting from the downregulation of CSE, CBS, and 3-MST under renal hypertensive conditions.

In addition, there is an urgent need to clarify the molecular mechanisms of H$_2$S in the baroreflex afferent pathway. Growing evidence suggests that PKA is a downstream target of H$_2$S [51]. The residue serine 897 on the NMDA receptor 1 (NR1) subunit is specifically phosphorylated by PKA [52]. In most neurons, increases in the levels of phosphorylated NR may result in increased function of the receptor [53], which leads to undebatable reflex hypotension. The NMDA receptor plays an important role in the regulation of NTS vagal afferent activity. Glutamate is known to be present in most vagal afferent terminals. In addition, the dendrites at the afferent ends of the vagus nerve contain NMDA receptors. Additionally, the injection of L-glutamate into the NTS can cause a depressor response, similar to the effect of baroreflex activation. Therefore, it is widely accepted that glutamate can regulate the baroreflex at the level of the NTS mediated at least partially through the PKA-NR1 signaling pathway. Thus, we focused on this pathway to verify the participation and baroreflex afferent mechanism of H$_2$S in neuromodulation. Our results confirmed that the expression of PKA and p-NR1 was exclusively regulated in the NG and NTS in the case of renovascular hypertension and mitigated in vivo by local H$_2$S treatment, which is supported by the finding that both PKA and NR1 are involved in baroreflex activity [54]. In addition, other studies reported that NMDA (0.5 pmol/100 nL) microinjection into the NTS decreased MAP and that cAMP/PKA transmitted hypotensive signals in the NTS of SHRs [55, 56]. Thus, upregulation of PKA/p-NR1 in the NG and NTS is likely to be due at least in part to negative feedback regulation under pathophysiological conditions. This also strongly suggests that p-NR1 upregulation under hypertensive conditions is due to a compensatory mechanism. Collectively, these data support the idea that the PKA/NR1 pathway may not be a direct target of H$_2$S in the baroreflex afferent pathway but may participate in improving BRS and BP.

The K$_{ATP}$ channel is an important downstream target of H$_2$S activity in central neurons responsible for its neuroprotective effects [57]. In particular, H$_2$S-induced cardiovascular functions in the baroreflex afferent pathway may be mediated by K$_{ATP}$ channel activation [47]. The present study clearly indicated that Gli, a K$_{ATP}$ channel blocker, can partially inhibit the effects of H$_2$S in decreasing BP and improving BRS. This observation was further confirmed by the microinjection of Gli into the NG, which significantly inhibited the antihypertensive effect of H$_2$S in the NG. The K$_{ATP}$ channel is present in a wide variety of organs, but the composition of its subunits varies depending upon the tissue. Neurons and pancreatic β cells carry channels mostly composed of the Kir6.2 and SUR1 subunits [58, 59]. Our further studies revealed that renovascular hypertension downregulated Kir6.2 and SUR1 expression in the baroreflex afferent pathway and that this effect could be reversed by chronic injection of NaHS, which echoed our previous results. Therefore, the obvious upregulation of BRS and reduction in BP induced by H$_2$S infusion in rats is partially related to the activation of K$_{ATP}$ channels in the NG and NTS.

In summary, the new findings of this investigation have confirmed that through K$_{ATP}$ channel activation, H$_2$S has a significant antihypertensive effect via novel and direct targets (the NG and NTS) within the baroreflex afferent pathway for the neurocontrol of BP regulation under physiological and hypertensive disease conditions.

REFERENCES
1. Reiffenstein RJ, Hulbert WC, Roth SH. Toxicology of hydrogen sulfide. Annu Rev Pharmacol Toxicol. 1992;32:109–34.
2. Wang R. Two's company, three's a crowd: can H₂S be the third endogenous gaseous transmitter? FASEB J. 2002;16:1792–8.
3. Kamat PK, Kalani A, Tyagi N. Role of hydrogen sulfide in brain synaptic remodeling. Methods Enzymol. 2015;555:207–29.
4. Nandi SS, Mishra PK. H2S and homocysteine control a novel feedback regulation of cystathionine beta synthase and cystathionine gamma lyase in cardiomyocytes. Sci Rep. 2017;7:3639.
5. Zhang M, Shan H, Chang P, Ma L, Chu Y, Shen X, et al. Upregulation of 3-MST relates to neuronal autophagy after traumatic brain injury in mice. Cell Mol Neurobiol. 2017;37:291–302.
6. De Cicco P, Panza E, Ercolano G, Armogida C, Sessa G, Pirozzi G, et al. ATB-346, a novel hydrogen sulfide-releasing anti-inflammatory drug, induces apoptosis of human melanoma cells and inhibits melanoma development in vivo. Pharmacol Res. 2016;114:67–73.
7. Wei HJ, Xu JH, Li MH, Tang JP, Zou W, Zhang P, et al. Hydrogen sulfide inhibits homocysteine-induced endoplasmic reticulum stress and neuronal apoptosis in rat hippocampus via upregulation of the BDNF-TrkB pathway. Acta Pharmacol Sin. 2014;35:707–15.
8. Liu F, Liu GJ, Liu N, Zhang G, Zhang JX, Li LF. Effect of hydrogen sulfide on inflammatory cytokines in acute myocardial ischemia injury in rats. Exp Ther Med. 2015;9:1068–74.
9. Zhang CY, Li XH, Zhang T, Fu J, Cui XD. Hydrogen sulfide suppresses the expression of MMP-8, MMP-13, and TIMP-1 in left ventricles of rats with cardiac volume overload. Acta Pharmacol Sin. 2013;34:1301–9.
10. Liu YH, Lu M, Hu LF, Wong PT, Webb GD, Bian JS. Hydrogen sulfide in the mammalian cardiovascular system. Antioxid Redox Signal. 2012;17:141–85.
11. Yang G, Wu L, Jiang B, Yang W, Qi J, Cao K, et al. H₂S as a physiologic vasorelaxant: hypertension in mice with deletion of cystathionine gamma-lyase. Science 2008;322:587–90.
12. Lu M, Liu YH, Goh HS, Wang JJ, Yong QC, Wang R, et al. Hydrogen sulfide inhibits plasma renin activity. J Am Soc Nephrol. 2010;21:993–1002.
13. Yu W, Liao Y, Huang Y, Chen SY, Sun Y, Sun C, et al. Endogenous hydrogen sulfide enhances carotid sinus baroreceptor sensitivity by activating the transient receptor potential cation channel subfamily V member 1 (TRPV1) channel. J Am Heart Assoc. 2017;6:e004971.
14. Liu Y, Zhou JY, Zhou YH, Wu D, He JL, Han LM, et al. Unique expression of angiotensin type-2 receptor in sex-specific distribution of myelinated Ah-type baroreceptor neuron contributing to sex-dimorphic neurocontrol of circulation. Hypertension. 2016;67:783–91.
15. Shan Z, Zubcevic J, Shi P, Jun JY, Dong Y, Murca TM, et al. Chronic knockdown of the nucleus of the solitary tract AT1 receptors increases blood inflammatory-endothelial progenitor cell ratio and exacerbates hypertension in the spontaneously hypertensive rat. Hypertension. 2013;61:1328–33.
16. Tsyrlin VA, Galagudza MM, Kuzmenko NV, Pliss MG, Rubanova NS, Shcherbin YI. Arterial baroreceptor reflex counteracts long-term blood pressure increase in the rat model of renovascular hypertension. PLoS ONE. 2013;8:e64788.
17. Zhao W, Zhang J, Lu Y, Wang R. The vasorelaxant effect of H₂S as a novel endogenous gaseous K$_{ATP}$ channel opener. EMBO J. 2001;20:6008–16.
18. Yang ZW, Li DJ, Liu C, Han P, Yang YL, Su DF, et al. Role of vascular K$_{ATP}$ channels in blood pressure variability after sinoaortic denervation in rats. Acta Pharmacol Sin. 2011;32:194–200.
19. Szeto V, Chen NH, Sun HS, Feng ZP. The role of K$_{ATP}$ channels in cerebral ischemic stroke and diabetes. Acta Pharmacol Sin. 2018;39:683–94.
20. Vazquez-Sanchez AY, Hinojosa LM, Parraguirre-Martinez S, Gonzalez A, Morales F, Montalvo G, et al. Expression of K$_{ATP}$ channels in human cervical cancer: potential tools for diagnosis and therapy. Oncol Lett. 2018;15:6302–8.
21. Wang JJ, Rong WF, Wang WZ, Zhang L, Yuan WJ. NMDA receptor mechanism involved in arterial baroreflex. Acta Pharmacol Sin. 2000;21:617–22.
22. Ying SH, Jing YA. A new method for establishing renovascular hypertensive rat model. J Xianning Med Coll. 1999;13:18–20.
23. Bartosiewicz J, Kaminski T, Pawlak K, Karbowska M, Tankiewicz-Kwedlo A, Pawlak D. The activation of the kynurenine pathway in a rat model with renovascular hypertension. Exp Biol Med. 2017;242:750–61.
24. Sikora M, Pham K, Ufnal M. Hypotensive effect of S-adenosyl-L-methionine in hypertensive rats is reduced by autonomic ganglia and K$_{ATP}$ channel blockers. Amino Acids. 2016;48:1581–90.
25. Arnold AC, Shaltout HA, Gallagher PE, Diz DI. Leptin impairs cardiovagal baroreflex function at the level of the solitary tract nucleus. Hypertension. 2009;54:1001–8.
26. Zhang D, Liu J, Tu H, Muelleman RL, Cornish KG, Li YL. In vivo transfection of manganese superoxide dismutase gene or nuclear factor kappaB shRNA in nodose ganglia improves aortic baroreceptor function in heart failure rats. Hypertension. 2014;63:88–95.
27. Zhang C, Du J, Bu D, Yan H, Tang X, Si Q, et al. The regulatory effect of hydrogen sulfide on hypoxic pulmonary hypertension in rats. Biochem Biophys Res Commun. 2003;302:810–6.
28. Yan H, Du JB, Tang CS. Changes and significance of hydrogen sulfide/cystathionine gamma-lyase system in hypertension: an experimental study with rats. Zhonghua Yi Xue Za Zhi. 2004;84:1114–7.
29. Bian JS, Yong QC, Pan TT, Feng ZN, Ali MY, Zhou S, et al. Role of hydrogen sulfide in the cardioprotection caused by ischemic preconditioning in the rat heart and cardiac myocytes. J Pharmacol Exp Ther. 2006;316:670–8.
30. Elrod JW, Calvert JW, Morrison J, Doeller JE, Kraus DW, Tao L, et al. Hydrogen sulfide attenuates myocardial ischemia-reperfusion injury by preservation of mitochondrial function. Proc Natl Acad Sci USA. 2007;104:15560–5.
31. Chiu HY, Lin HH, Lai CC. Potentiation of spinal NMDA-mediated nociception by cocaine- and amphetamine-regulated transcript peptide via PKA and PKC signaling pathways in rats. Regul Pept. 2009;158:77–85.
32. Xu M, Wu YM, Li Q, Liu S, Li Q, He RR. Electrophysiological effects of hydrogen sulfide on human atrial fibers. Chin Med J. 2011;124:3455–9.
33. Grassi G. Assessment of sympathetic cardiovascular drive in human hypertension: achievements and perspectives. Hypertension. 2009;54:690–7.
34. Guo GB, Abboud FM. Impaired central mediation of the arterial baroreflex in chronic renal hypertension. Am J Physiol. 1984;246:H720–H727.
35. El-Sayed SS, Zakaria MN, Abdel-Ghany RH, Abdel-Rahman AA. Cystathionine-gamma lyase-derived hydrogen sulfide mediates the cardiovascular protective effects of moxonidine in diabetic rats. Eur J Pharmacol. 2016;783:73–84.
36. Li H, Teng X, Yang R, Guo Q, Xue H, Xiao L, et al. Hydrogen sulfide facilitates the impaired sensitivity of carotid sinus baroreflex in rats with vascular calcification. Front Pharmacol. 2017;8:629.
37. Xiao L, Wu YM, Zhang H, Liu YX, He RR. Hydrogen sulfide facilitates carotid sinus baroreflex in anesthetized rats. Acta Pharmacol Sin. 2006;27:294–8.
38. Koomans HA, Blankestijn PJ, Joles JA. Sympathetic hyperactivity in chronic renal failure: a wake-up call. J Am Soc Nephrol. 2004;15:524–37.
39. Pliquett RU, Benkhoff S, Jung O, Brandes RP. Sympathoactivation and rho-kinase-dependent baroreflex function in experimental renovascular hypertension with reduced kidney mass. BMC Physiol. 2014;14:4.
40. Tromp TR, Mahesh D, Joles JA, Ramchandra R. Direct recording of cardiac and renal sympathetic nerve activity shows differential control in renovascular hypertension. Hypertension. 2018;71:1108–16.
41. Drazner MH. The progression of hypertensive heart disease. Circulation. 2011;123:327–34.
42. Sun NL, Xi Y, Yang SN, Ma Z, Tang CS. Plasma hydrogen sulfide and homocysteine levels in hypertensive patients with different blood pressure levels and complications. Zhonghua Xin Xue Guan Bing Za Zhi. 2007;35:1145–8.
43. Sun L, Sun S, Li Y, Pan W, Xie Y, Wang S, et al. Potential biomarkers predicting risk of pulmonary hypertension in congenital heart disease: the role of homocysteine and hydrogen sulfide. Chin Med J. 2014;127:893–9.
44. Wang C, Han J, Xiao L, Jin CE, Li DJ, Yang Z. Role of hydrogen sulfide in portal hypertension and esophagogastric junction vascular disease. World J Gastroenterol. 2014;20:1079–87.
45. Ahmad FU, Sattar MA, Rathore HA, Tan YC, Akhtar S, Jin OH, et al. Hydrogen sulphide and tempol treatments improve the blood pressure and renal excretory responses in spontaneously hypertensive rats. Ren Fail. 2014;36:598–605.
46. Liu WQ, Chai C, Li XY, Yuan WJ, Wang WZ, Lu Y. The cardiovascular effects of central hydrogen sulfide are related to K$_{ATP}$ channels activation. Physiol Res. 2011;60:729–38.

47. Qiao W, Yang L, Li XY, Cao N, Wang WZ, Chai C, et al. The cardiovascular inhibition functions of hydrogen sulfide within the nucleus tractus solitarii are mediated by the activation of K_{ATP} channels and glutamate receptors mechanisms. Pharmazie. 2011;66:287–92.

48. Liu Y, Wu D, Qu MY, He JL, Yuan M, Zhao M, et al. Neuropeptide Y-mediated sex- and afferent-specific neurotransmissions contribute to sexual dimorphism of baroreflex afferent function. Oncotarget. 2016;7:66135–48.

49. Yuan M, Ma MN, Wang TY, Feng Y, Chen P, He C, et al. Direct activation of tachykinin receptors within baroreflex afferent pathway and neurocontrol of blood pressure regulation. CNS Neurosci Ther. 2019;25:123–35.

50. Wen X, Yu X, Huo R, Yan QX, Wu D, Feng Y, et al. Serotonin-mediated cardiac analgesia via Ah-type baroreceptor activation contributes to silent angina and asymptomatic infarction. Neuroscience. 2019;411:150–63.

51. Jiang LH, Wang J, Wei XL, Liang QY, Cheng TT. Exogenous sodium hydrosulfide can attenuate naloxone-precipitated withdrawal syndromes and affect cAMP signaling pathway in heroin-dependent rat's nucleus accumbens. Eur Rev Med Pharmacol Sci. 2012;16:1974–82.

52. Ron D. Signaling cascades regulating NMDA receptor sensitivity to ethanol. Neuroscientist. 2004;10:325–36.

53. Chen BS, Roche KW. Regulation of NMDA receptors by phosphorylation. Neuropharmacology. 2007;53:362–8.

54. Chan SH, Chang KF, Ou CC, Chan JY. Up-regulation of glutamate receptors in nucleus tractus solitarii underlies potentiation of baroreceptor reflex by heat shock protein 70. Mol Pharmacol. 2002;61:1097–104.

55. Dias AC, Vitela M, Colombari E, Mifflin SW. Nitric oxide modulation of glutamatergic, baroreflex, and cardiopulmonary transmission in the nucleus of the solitary tract. Am J Physiol Heart Circ Physiol. 2005;288:H256–H262.

56. Tai MH, Weng WT, Lo WC, Chan JY, Lin CJ, Lam HC, et al. Role of nitric oxide in alpha-melanocyte-stimulating hormone-induced hypotension in the nucleus tractus solitarii of the spontaneously hypertensive rats. J Pharmacol Exp Ther. 2007;321:455–61.

57. Wang JF, Li Y, Song JN, Pang HG. Role of hydrogen sulfide in secondary neuronal injury. Neurochem Int. 2014;64:37–47.

58. Schiffrin EL, Park JB, Intengan HD, Touyz RM. Correction of arterial structure and endothelial dysfunction in human essential hypertension by the angiotensin receptor antagonist losartan. Circulation. 2000;101:1653–9.

59. Liss B, Roeper J. Molecular physiology of neuronal K_{ATP} channels. Mol Membr Biol. 2001;18:117–27.